NEOPLASIA
283
www.neoplasia.com

Volume 22 Number 8 August 2020 pp. 283–293

WHSC1 monomethylates histone H1 and induces stem-cell like features in squamous cell carcinoma of the head and neck

Vassiliki Saloura [a,*,1]; Theodore Vougiouklakis [b,1]; Riyue Bao [c,d]; Sohyoung Kim [e]; Songjoon Baek [e]; Makda Zewde [b]; Benjamin Bernard [a]; Kyunghee Burkitt [a]; Nupur Nigam [a]; Evgeny Izumchenko [b]; Naoshi Dohmae [h]; Ryuji Hamamoto [f]; Yusuke Nakamura [b,g]

[a] Thoracic and GI Malignancies Branch, Center for Cancer Research, National Cancer Institute, Bethesda, USA; [b] Department of Medicine, University of Chicago, Chicago, USA; [c] Center for Research Bioinformatics, University of Chicago, Chicago, USA; [d] Department of Pediatrics, University of Chicago, Chicago, USA; [e] Laboratory of Receptor Biology and Gene Expression, National Cancer Institute, USA; [f] National Cancer Center Research Institute, Tokyo, Japan; [g] Department of Surgery, University of Chicago, Chicago, USA; [h] Biomolecular Characterization Unit, RIKEN, Japan

Abstract

Squamous cell carcinoma of the head and neck (SCCHN) is a malignancy with poor outcomes, thus novel therapies are urgently needed. We recently showed that WHSC1 is necessary for the viability of SCCHN cells through H3K36 di-methylation. Here, we report the identification of its novel substrate, histone H1, and that WHSC1-mediated H1.4K85 mono-methylation may enhance stemness features in SCCHN cells. To identify proteins interacting with WHSC1 in SCCHN cells, WHSC1 immunoprecipitation and mass spectrometry identified H1 as a WHSC1-interacting candidate. In vitro methyltransferase assays showed that WHSC1 mono-methylates H1 at K85. We generated an H1K85 mono-methylation-specific antibody and confirmed that this methylation occurs in vivo. Sphere formation assays using SCC-35 cells stably expressing either wild-type (FLAG-H1.4-WT) or mutated (FLAG-H1.4K85A) vector with lysine 85 to alanine substitution which is not methylated, indicated a higher number of spheres in SCC-35 cells expressing the wild type than those with the mutant vector. SCC-35 cells expressing the wild type H1.4 proliferated faster than those expressing the mutated vector. RNA sequencing, RT-PCR and Western blotting of the FLAG-H1.4-WT or FLAG-H1.4K85A SCC-35 cells revealed that OCT4 levels were higher in wild type compared to mutant cells. These results were reproduced in SCC-35 cells genetically modified with CRISPR to express H1.4K85R. Chromatin immunoprecipitation showed that FLAG-H1.4K85A had decreased occupancy in the OCT4 gene compared to FLAG-H1.4-WT. This study supports that WHSC1 mono-methylates H1.4 at K85, it induces transcriptional activation of OCT4 and stemness features in SCCHN cells, providing rationale to target H1.4K85 mono-methylation through WHSC1 in SCCHN.

Neoplasia (2020) 22 283–293

Keywords: WHSC1, Histone H1, Squamous cell carcinoma of the head and neck, Methylation

Introduction

Histones are positively charged nuclear proteins that package DNA into chromatin. They are categorized mainly as the core histones H2A, H2B, H3 and H4, which comprise the octameric nucleosome core particles, and the lysine-rich linker H1 histones. H1 binds to the nucleosome and the linker DNA region at the entry/exit of the nucleosomes, forming the next structural unit of chromatin, the chromatosome. Linker H1 histones are a heterogeneous family of proteins with tissue-specific expression patterns, and they are characterized by a similar tripartite structure made of a short N-terminal domain, a central globular domain and a longer C-terminal domain. The N-terminal and the globular domains are conserved among the H1 family members, whereas the C-terminal domains show significant differences. The globular and C-terminal domains of H1 are the main determinants for H1 binding to DNA, which is mainly mediated by positively charged arginine and lysine residues with

* Corresponding author.
e-mail address: vassiliki.saloura@nih.gov (V. Saloura).
[1] Equally contributed.

https://doi.org/10.1016/j.neo.2020.05.002

the phosphate groups of the DNA backbone [1]. There are eleven different variants of human H1, each one encoded by a different gene. Five of these variants are replication-independent and are encoded by genes scattered throughout the genome. Six of the genes are replication-dependent, including H1.1 (*HIST1H1A*), H1.2 (*HIST1H1C*), H1.3 (*HIST1H1D*), H1.4 (*HIST1H1E*) and H1.5 (*HIST1H1B*). H1.1–H1.5 are expressed in most of somatic cells and their respective genes reside within the histone gene cluster 1 on chromosome 6p region. H1.4 is the predominant histone variant expressed in most cell types. Despite their similarities in their amino-acid sequence, H1 variants are thought to possess different functions and affinities to different chromatin regions, and this is supported by the different phenotypes and gene expression patterns that are seen in H1-variant knockdown cellular models [2].

In normal cells, linker histones influence nucleosome positioning and spacing, the degree of chromatin compaction, the structural integrity of chromosomes during mitosis, and the stability and maintenance of higher order chromatin structure ([3,4,5]). More specifically, binding of H1 to linker DNA is known to lead to a more compacted chromatin, thus decreasing the accessibility of regulatory proteins, chromatin remodeling factors and histone modifiers to DNA. H1 has also been reported to regulate transcription either by repression or activation of specific genes [2]. During the S-phase, H1 phosphorylation, which mimics H1 depletion and resultant decondensation, has also been reported to halt progression to mitosis [6]. Additionally, linker histones play a vital role in embryonic development and cellular differentiation [7]. This is supported by Zhang et al. [8], who showed that depletion of histone H1 impaired embryonic stem cell differentiation and that H1 might mediate pluripotent stem cell differentiation through epigenetic silencing of pluripotency genes. Furthermore, [9] reported that citrullination of histone H1, which leads to looser association of H1 with DNA, is an essential component of pluripotency. In addition, H1.2 has been shown to induce apoptosis mediated by irradiation and its depletion leads to resistance to apoptosis [10]. In another study, Garg et al. [11] suggested that the C-terminal region of linker histones is necessary and sufficient for a proapoptotic function of linker histones. Linker histones are subject to extensive posttranslational modifications (PTMs), such as phosphorylation, acetylation, ADP-ribosylation and methylation, however the respective histone modifiers and the relevant biological functions are not well defined yet [12,13].

Other than their physiologic role, recent reports have also suggested association of linker histones with various cancer processes. Chadee et al. [14] reported that phosphorylation of H1 activates the Ras signaling pathway which is a known driver of oncogenesis. Embryonic stem cells from H1c, H1d and H1e (analogous to human H1.2, H1.3 and H1.4 respectively) triple-knockout mice, characterized by loose chromatin, were also found to be hyper-resistant to DNA-damaging agents due to hyperactive DNA-damage response [15]. More recently, the Cancer Genome Atlas project (TCGA) revealed multiple genomic aberrations in linker histones in the majority of cancer types, with frequencies ranging from approximately 6% to 12% in pancreatic, cervical, head and neck and colorectal cancers [16,17]. Li et al. [17] also reported recurrent mutations in linker histone genes in follicular lymphoma, implicating linker histones in the epigenetic deregulation of lymphoma. Still, the specific pathogenetic pathways involving linker histones with cancer are largely elusive.

Squamous cell carcinoma of the head and neck (SCCHN) is a significant public health concern affecting over 50,000 patients annually in the United States [18]. Cisplatin-based chemoradiotherapy and cetuximab, an antibody targeting the epidermal growth factor receptor (EGFR), are standard treatments, but many patients eventually develop resistance, thus the development of new therapies is urgently needed. The TCGA recently revealed a plethora of genetic and expression aberrations in multiple histone modifiers in SCCHN. One of these histone modifiers is Wolf-Hirschhorn syndrome candidate 1 (WHSC1), a protein lysine methyltransferase which is known to di- and tri-methylate lysine on position 36 of histone H3 (H3K36). We recently showed that WHSC1 is significantly and frequently overexpressed in tumors of locoregionally advanced SCCHN, its overexpression was associated with poor differentiation and was necessary for the survival of SCCHN cells partially through transcriptional upregulation of the cell cycle related gene NIMA-related kinase 7 (NEK7) [19]. This effect was mediated through induction of di-methylation of H3K36 at the gene body region of NEK7. In this report, we show that WHSC1 binds and directly monomethylates lysine 85 in the conserved globular DNA-binding region of linker histone H1, and that this methylation is critical for stemness features in SCCHN cells. In the context of ongoing efforts for the development of a WHSC1 inhibitor, this report provides further mechanistic insight and biological rationale for the introduction of WHSC1-inhibitors in clinical trials for patients with SCCHN.

Materials and methods

Cell culture and generation of SCC-35 stable cells expressing FLAG-H1.4-WT or FLAG-H1.4K85A

Squamous cell carcinoma cells SCC-35 were derived from a patient with locoregionally advanced SCCHN of the pyriform sinus (T4N0, HPV-negative, TP53 wild-type) and were kindly provided by Dr. Tanguy Seiwert (University of Chicago). Parental SCC-35 cells were maintained in DMEM/F12 medium with 10% fetal bovine serum, 1% penicillin/streptomycin, and 2 nM L-glutamine. HELA cells were commercially obtained and maintained in DMEM medium with 10% fetal bovine serum and 1% penicillin/streptomycin. PE/CA-PJ15 cells (HPV-negative, tongue) were maintained in IDMEM medium with 10% fetal bovine serum, 1% penicillin/streptomycin, and 2 nM L-glutamine. FaDu cells (HPV-negative, hypopharynx) were maintained in RPMI medium with 10% fetal bovine serum, 1% penicillin/streptomycin, and 2 nM L-glutamine. All cell lines were maintained at 37 °C in humid air with 5% CO2 condition. To generate SCC-35 cells stably expressing FLAG-H1.4-WT or FLAG-H1.4K85A, SCC-35 cells were transfected with FuGENE HD (Roche Applied Science, Madison, WI) according to manufacturer's protocols with the FLAG-H1.4-WT versus FLAG-H1.4K85A versus FLAG-Mock pcDNA3.1 vectors. After 48 h of transfection, cells were exposed to G418 (1 μg/μL) and appropriate cell death was observed after 1 week of G418 exposure. Bulk selection was then performed for each of the three stable cell lines. Subsequently, stably transfected SCC-35 cells grew well and were maintained in DMEM/F12 medium with 10% fetal bovine serum, 1% penicillin/streptomycin and 1μg/μL G418. All experiments involving SCC-35 stably transfected cells were performed using cells that were passaged up to a maximum of 7 times.

Cell culture and generation of SCC-35-H1.4K85R cells

The generation of SCC-35-H1.4K85R cells using CRISPR was outsourced by Applied Stem Cell. The introduction of the H1.4K85R mutation in SCC-35 cells was confirmed by Sanger sequencing. SCC-35-H1.4K85R cells were maintained in DMEM/F12 medium with 10% fetal bovine serum, 1% penicillin/streptomycin, and 2 nM L-glutamine, as parental SCC-35 cells.

Expression vector construction

Vectors expressing N-terminal HA- and FLAG-tagged wild-type H1.4 and mutant H1.4K85A proteins were constructed by Genscript using a pcDNA3.1(+) backbone. Cloning of the coding sequence of wild-type

H1.4 was performed in the HindIII-BamHI cloning site of the pcDNA3.1 (+) backbone vector, followed by mutagenesis to obtain the H1.4K85A expressing vector. Sanger sequencing was conducted to confirm the plasmid DNA sequence.

Sphere formation assay

5000 SCC-35 stably transfected cells were seeded in 24-well low-attachment plates in serum-free medium supplemented by epidermal growth factor (20 ng/ml), 1% penicillin/streptomycin and G418 (1 μg/μL). Cells were followed for 7 days and spheres were counted in each well for each condition. Number of spheres were counted in 3 separate wells per condition under the microscope and the mean number of spheres was calculated.

RNA isolation and RNA sequencing of SCC-35 cells stably expressing FLAG-H1.4-WT or FLAG-H1.4K85A, parental SCC-35 and SCC-35-H1.4K85R cells

RNA was isolated from SCC-35 cells stably expressing FLAG-H1.4-WT or FLAG-H1.4K85A using the AllPrep DNA/RNA kit (Qiagen, Venlo, Netherlands). RNA sequencing of samples with at least 1ug of RNA was outsourced by Theragen Etex. 1 sample per condition was sequenced. More specifically, RNA quality was assessed by analysis of rRNA band integrity on an Agilent RNA 6000 Nano kit (Agilent Technologies, CA). For the cDNA library construction, 1 μg of total RNA and magnetic beads with oligo (dT) were used to enrich poly (A) mRNA from it. Then, the purified mRNAs were disrupted into short fragments and double-stranded cDNAs were immediately synthesized. The cDNAs were subjected to end-repair, poly (A) addition, and connected with sequencing adapters using the TruSeq RNA sample prep Kit (Illumina, CA). Suitable fragments that were automatically purified by BluePippin 2% agarose gel cassette (Sage Science, MA) were selected as templates for PCR amplification. The final library sizes and quality were evaluated electrophoretically with an Agilent High Sensitivity DNA kit (Agilent Technologies, CA) and the fragments were found to be between 350–450 bp. Subsequently, the library was sequenced using an Illumina HiSeq2500 sequencer (Illumina, CA).

Similarly, RNA was isolated from parental SCC-35 and SCC-35-H1.4K85R cells, and RNA libraries (stranded) were constructed in 3 biological replicates from each cell line following the above described procedure and sequenced using Illumina NextSeq 500 with 2 × 76 bp. The RNA-seq data from the parental SCC-35 and SCC-35-H1.4K85R cells were analyzed following protocols as previously described [24]. In brief, after quality assessment, paired-end sequence reads were aligned to human reference transcriptome with GENCODE gene annotation (v29, GRCh38 primary assembly) [25] by Kallisto in the strand-specific mode (v0.45.0). Transcript-level expression was quantified and subsequently summarized into gene level using tximport (v1.10.1), normalized by trimmed mean of *M* values (TMM) method, and log2-transformed. Genes expressed (defined as, counts per million of mapped reads (CPM) >3) in at least three samples were kept for further analysis. Genes differentially expressed between groups were identified using the limma voom algorithm (v3.38.3) and filtered at FDR-corrected $p < 0.10$ and fold change ≥ 1.5 or ≤ -1.5. Gene Ontology (GO) and Kyoto Encyclopedia of Genes and Genomes (KEGG) pathways significantly enriched in the genes of interest were identified using clusterprofiler (v3.10.1) at FDR-corrected $p < 0.10$ (hypergeometric test). Gene Set Enrichment Analysis (GSEA) was performed with Hallmark gene sets (H) from the Molecular Signature Database (MSigDB) database (v6.2) using R package fGSEA (v1.8.0) at FDR-corrected $p < 0.10$. The statistical significance of the enrichment score was computed using the default software settings and 10,000 permutations. BH-FDR method was used for multiple testing correction.

RT-PCr

RNA was isolated using the AllPrep DNA/RNA kit (Qiagen, Venlo, Netherlands) from stably transfected, parental SCC-35 cells and SCC-35-H1.4K85R cells. Specific primers for human *GAPDH* (housekeeping gene) and *OCT4* were designed (primer sequences in Supplementary Table S1). PCR reactions were performed using ViiA 7 real-time PCR system (Thermo Fisher Scientific, Waltham, MA) following the manufacture's protocol.

siRNA transfection

MISSION_ siRNA oligonucleotide duplexes were purchased from Sigma–Aldrich for targeting the human WHSC1 transcripts. siNegative control (siNC), which consists of three different oligonucleotide duplexes, were used as control siRNAs (Cosmo Bio, Tokyo, Japan). The siRNA sequences are described in Supplementary Table S2. SCC-35 SCCHN cells were plated overnight in 10 cm dishes and were transfected with siRNA duplexes (50 nM final concentration) using Lipofectamine RNAimax (Life Technologies) for 72 h. Cells were then collected and nuclear extraction was performed (Active Motif), followed by Western blotting as described below.

Cell growth assays

SCC-35 stably transfected cells (FLAG-H1.4-WT versus FLAG-H1.4K85A) were plated in quadruples at a seeding density of 2000 cells/well in 24-well plates. The number of viable cells was measured using the Cell Counting Kit-8 (Dojindo, Kumamoto, Japan) on the indicated time points.

Western blotting

Nuclear extracts were prepared using the Nuclear Extraction kit (Active Motif) to examine protein levels of WHSC1, FLAG-tagged wild-type and mutant H1.4 and histone H3. Samples were prepared from the cells lysed with CelLytic M cell lysis reagent (Sigma-Aldrich) containing a complete protease inhibitor cocktail (Roche Applied Science), and whole cell lysates or immunoprecipitation (IP) products were transferred to nitrocellulose membrane. Protein bands were detected by incubating with horseradish peroxidase (HRP)-conjugated antibodies (GE Healthcare) and visualized with enhanced chemiluminescence (GE Healthcare). We declare that our blots were evenly exposed in each membrane and that the blots were not cropped to the bands. Primary antibodies were used as described in the ``Antibodies'' section.

Immunoprecipitation

UD-SCC-2 cells (T2N1, hypopharynx, HPV-positive, TP53 wild-type) or transfected HELA cells were lysed with CelLytic M cell lysis reagent (Sigma Aldrich) containing a complete protease and phosphatase inhibitor cocktail (Roche Applied Science). In a typical IP reaction, 300–800 μg of whole-cell extract was incubated with an optimum concentration of primary antibody. After the protein G beads had been washed three times in 1 ml of TBS buffer (pH 7.6), proteins that bound to the beads were eluted by boiling in Lane Marker Reducing Sample Buffer (Thermo Scientific).

Immunocytochemistry

SCC-35 cells stably expressing FLAG-H1.4-WT, FLAG-H1.4K85A or control FLAG-pcDNA3.1(+) were seeded at 50,000 cells per well in 4-well chambers with G418 at 1 μg/μL in 1 ml of DMEM/F12 medium supplemented with 10% fetal bovine serum, 1% penicillin/streptomycin and 2 nM of L-glutamine. After 24 h, medium was removed and cells were washed 2 times with 1 ml of PBS. Following suctioning of PBS, 1 ml of 4% paraformaldehyde was added to each well for 30 min at 4 °C to fix the cells. Subsequently cells were washed with PBS three times for 5 min each time at room temperature. 0.1% Triton X-100 was added for 3 min at room temperature to permeabilize the cells and samples were washed with PBS three times for 5 min each time. Then cells were blocked with 3% BSA for 1 h at room temperature and incubated with primary anti-FLAG M2 mouse antibody (Sigma-Aldrich, F3165) in a 1 ml solution of 3% BSA at 4 °C overnight. Next day, cells were washed 4 times with 1 ml of PBS and secondary antibody was added (anti-mouse Alexa 488, dilution: 1:1000) for 1 h at RT with gentle shaking. Following this, cells were washed 4 times with PBS and mounting medium with DAPI (VECTASHIELD®, Vector Laboratories) was added on each well. The wells were finally covered with a glass slide. Confocal microscopy (Leica 2D-Photon microscope) was used for the observation of stained cells. ImageJ software was used to analyze the images.

Antibodies

Primary antibodies used were anti-WHSC1 (mouse, Abcam, #75359, dilution used in WB: 1:5000), anti-FLAG (rabbit, F7425; Sigma-Aldrich; dilution used in WB: 1:20,000), anti-FLAG (mouse, F3165; Sigma-Aldrich; dilution used in immunocytochemistry: 1:2000), anti-HA (rabbit, H6908, Sigma-Aldrich; dilution used in WB: 1:2000), anti-H1.4 (rabbit, H7665, Sigma-Aldrich; dilution used in WB: 1:5000), anti-H1.4K85me1 (rabbit, customized antibody, Sigma-Aldrich, Japan, dilution used in WB: 1:1000), anti-OCT4 (rabbit, abcam 18976, dilution used in WB: 1:1000), anti-ACTB (mouse, A5441, Sigma-Aldrich, dilution used in WB: 1:5000), anti-H3 (rabbit, ab1791, abcam, dilution used in WB: 1:50,000), anti-H1.1 (rabbit, abcam 17584, dilution used in WB: 1:1000), anti-H1.2 (rabbit, abcam 17677, dilution used in WB: 1:1000), anti-H1.3 (rabbit, abcam 24174, dilution used in WB: 1:1000), anti-H1.4 (rabbit, Sigma-Aldrich H7665, dilution used in WB: 1:1000), anti-H1.5 (rabbit, abcam 24175, dilution used in WB: 1:1000).

In vitro methyltransferase assays

For the *in vitro* methyltransferase assay, recombinant H1 (1 μg/μL, 31.25 μM, EMD-Millipore, 32 kDa, #14-155) was incubated with recombinant WHSC1 enzyme (Active Motif, 0.5 μg/μL, 3.8 μM, 130 kDa) using 1 mCi S-adenosyl-L-[methyl-3H]-methionine (SAM; PerkinElmer) as the methyl donor in a mixture of 30 μL of methylase activity buffer (50 mM Tris-HCl at pH8.8, 10 mM dithiothreitol and 10 mM $MgCl_2$) overnight at 30 °C. Proteins were separated on a 5–20 % SDS–PAGE gel (Ready Gel; Bio-Rad), then transferred on a PVDF membrane and visualized by MemCode Reversible Stain (ThermoFisher Scientific) and fluorography.

Chromatin immunoprecipitation followed by RT-PCR

ChIP assays were performed using stably or transiently transfected SCC-35 cells expressing FLAG-H1.4-WT versus FLAG-H1.4K85A. Briefly, protein-DNA crosslinking was performed by adding HCHO directly to the culture medium to a final concentration of 1%. Cells were incubated for 10 min at RT and then 20× glycine was added for 5 min at RT. Medium was then suctioned and cells were washed with cold PBS containing protease inhibitors. Cells were scraped and centrifuged for 5 min at 1500 rpm. Pellets were then resuspended with 1% SDS CHIP lysis buffer and incubated on ice for 1 h. Cells were sonicated using the Diagenode for 15 cycles, 15 sec ON/15 sec OFF with medium energy. Samples were centrifuged for 10 min at 14,000 rpm at 4 °C and the supernatant was diluted 5-fold with CHIP dilution buffer containing protease inhibitors. Approximately 800 μg of chromatin were used for the CHIP-assay using the WHSC1 antibody using stably transfected cells, and approximately 140 μg for the CHIP-assay using the FLAG antibody using transiently transfected cells. Samples were first pre-cleared with Invitrogen Dynabeads M-280 (mouse #11201D, rabbit #11203D) and then treated with 20 μg of anti-WHSC1 (Abcam, #753559) or 20 μg of the anti-FLAG (Sigma Aldrich, #F3165) overnight at 4 °C with rotation. Next day, 100 μL of mouse or rabbit Dynabeads were added and samples were incubated at 4 °C for 2 h. Samples were placed in a magnetic rack and the protein-DNA/primary antibody/bead complexes were washed one time for 10 min and sequentially with 1 ml of low salt immune complex wash buffer, high salt immune complex wash buffer, LiCi immune complex wash buffer and then two times with TE buffer. After the last wash, samples were placed on the magnetic rack, supernatant was removed and reversal mix (5 M NaCl, 1 M Tris-HCl, 0.5 M EDTA, proteinase K, SDS 10%) was added. Samples were incubated overnight at 65 °C, and next day DNA was extracted with phenol–chloroform precipitation. DNA fragments were quantified for *OCT4* gene enrichment using RT-PCR and *OCT4* CHIP grade primers (Supplementary Table S2.

Micrococcal nuclease assay

Stably transfected SCC-35 cells were digested with 0.25 Units of micrococcal nuclease according to the EZ nucleosomal DNA Prep Kit (Zymo Research, Irvine, CA). Briefly, cell nuclei were isolated from 3.8×10^5 SCC-35 cells expressing either FLAG-H1.4-WT or FLAG-H1.4K85A and treated with 0.25 Units of micrococcal nuclease for 5 min at room temperature. The reaction was stopped and nucleosomes were purified and loaded in a 2% agarose gel.

Results

WHSC1 interacts with the linker histone H1 in SCCHN cells and directly monomethylates it at lysine K85 both in vitro and in vivo.

To decipher additional mechanisms other than H3K36 di-methylation through which WHSC1 promotes survival in SCCHN cells, we sought to identify proteins that interact with WHSC1. For this purpose, endogenous immunoprecipitation of WHSC1 was performed using nuclear cell lysates of UD-SCC-2 cells which overexpress WHSC1 (Fig. 1A), followed by protein electrophoresis and silver staining. Results revealed a number of bands which were more intense in the WHSC1-immunoprecipitate compared to the control IgG (Fig. 1B). We chose seven of these bands and analyzed them by liquid chromatography/mass spectrometry (LC/MS) (Supplementary Data, MS results). Analysis of the band corresponding to approximately 35kD revealed different linker histone H1 variants and we chose to further investigate these as candidate interacting proteins of WHSC1.

To assess whether WHSC1 directly methylates H1, *in vitro* methyltransferase assay of recombinant WHSC1 and H1 proteins was performed and revealed methylation of histone H1 by WHSC1 (Fig. 1C). To confirm that WHSC1 methylates H1 and to identify a specific methylated amino-acid residue(s), samples of the above reaction were further analyzed with LC/MS. Results showed that WHSC1 mono-methylates the lysine residue at position 85 in the globular domain of different linker histone H1 variants (H1.1, H1.2, H1.4, H1.5) (Fig. 1D). The protein expression

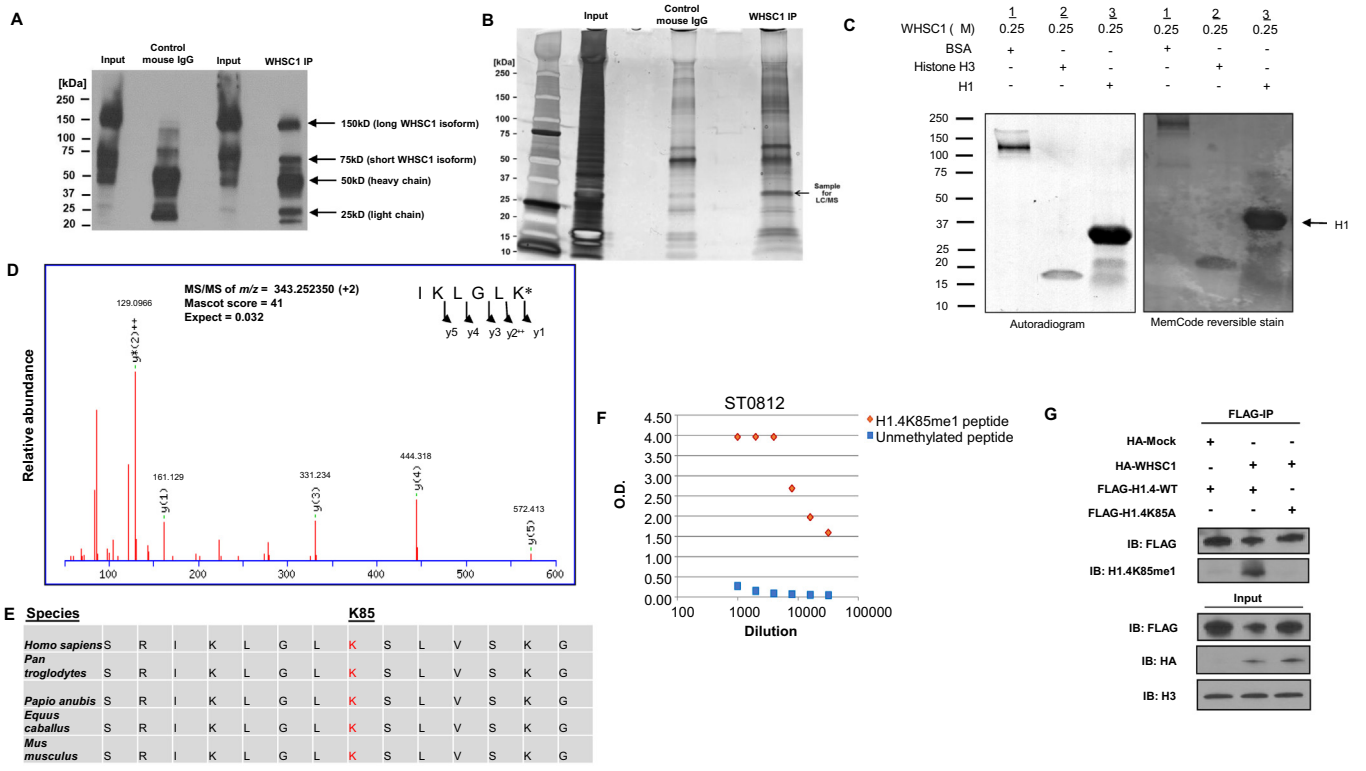

Fig. 1. WHSC1 interacts with histone H1 in nuclear extracts of UD-SCC-2 cells and directly mono-methylates it at lysine K85 *in vitro* and *in vivo*. A. Western blotting of endogenous immunoprecipitates for WHSC1 from 700 μg of nuclear extract (Active Motif kit) using the anti-WHSC1 mouse Abcam 75359 at 5 μg. Supernatants were denaturated with 5× sample buffer and heating of immunoprecipitate at 95 °C for 5 min. Normal mouse IgG was used as control for IP. B. Silver staining of nuclear extracts from UD-SCC-2 cells. Band indicated with arrow was analyzed by liquid chromatography-mass spectrometry. C. *In vitro* methyltransferase assay of recombinant WHSC1 with linker histone H1. Recombinant histone H1 (37 kD) was incubated with WHSC1 (130 kD) in the presence of ^{3}H-SAM. Bovine serum albumin (BSA, 66 kD) was used as a negative control and recombinant histone H3 (17 kD) as a positive control. The reactants were analyzed by SDS–PAGE followed by fluorography for 3 days (left panel). The PVDF transfer membrane was then stained with MemCode reversible protein stain to visualize the total protein (right panel). D. The MS/MS spectrum corresponding to the mono-methylated histone H1 fragment IKLGLK (79–85). The mono-methylation corresponds to lysine (K) at position 85 within the globular domain of histone H1. MS/MS score, Mascot ion score and Expectation value in Mascot Database search results are shown. E. Amino acid sequence alignment of human linker histone H1.4. The IKLGLK sequence which includes lysine K85 is located within the globular domain of H1 and is preserved from *Homo sapiens* to *Mus musculus*. F. Evaluation of the specificity of anti-mono-methylated K85 H1.4 antibody using enzyme-linked immunosorbent assay (ELISA). Y-axis represents ELISA optical density (OD) units read at 492 nm. ELISA plates coated with the mono-methylated K85 H1.4 peptide versus the unmodified H1.4 peptide were incubated with the primary rabbit antisera for 16 h at 4 °C (ST0812, Sigma-Aldrich, Japan). Detection was performed using a secondary rabbit antibody conjugated with horseradish peroxidase. Primary rabbit antisera were examined after dual selection against the modified versus the unmodified peptides. G. HeLa cells co-transfected with HA-Mock and FLAG-H1.4-WT versus HA-WHSC1 and FLAG-H1.4-WT or HA-WHSC1 and FLAG-H1.4K85A. FLAG-immunoprecipitation was performed using an anti-FLAG antibody and immunoprecipitates were blotted with the H1.4K85me1 and anti-FLAG antibodies. The input was blotted with anti-FLAG, anti-HA and anti-H3 antibodies.

levels of histone H1 variants were then examined in a panel of SCCHN cell lines and we found that H1.2 and H1.4 were the most abundantly expressed variants (Supplementary Fig. S1). Because the H1.4 variant is known to be the most abundantly expressed histone H1 variant in somatic cells, we decided to further study the H1.4 protein. Furthermore, the high conservation of K85 of H1.4 from *Homo sapiens* to *Mus musculus* (Fig. 1E) underlines a possible biologically significant role of its mono-methylation.

To investigate the presence of H1.4K85 mono-methylation (H1.4K85me1) in living cells, a customized antibody (ST0812) targeting K85 mono-methylated H1.4 was generated using a synthetic peptide flanking the mono-methylated lysine K85. The specificity of this antibody was first evaluated using an enzyme-linked immunosorbent assay (ELISA), testing the antibody against an ELISA plate coated with either the modified H1.4K85me1 or the unmodified H1.4 peptide (Fig. 1F). The specificity of the H1.4K85me1 antibody was further confirmed with an *in vitro* methyltransferase assay of recombinant histone H1 and bovine serum albumin versus recombinant WHSC1 (Supplementary Fig. S2). To assess whether the H1.4K85 mono-methylation occurs in living cells and to further confirm the specificity of the ST0812 antibody, we constructed a wild type FLAG-tagged H1.4 vector (FLAG-H1.4-WT) and a FLAG-tagged H1.4 vector with substitution of lysine K85 for alanine (FLAG-H1.4K85A). Then, we cotransfected HeLa cells with HA-Mock and FLAG-H1.4-WT, HA-WHSC1 and FLAG-H1.4-WT or HA-WHSC1 and FLAG-H1.4K85A vectors, and performed FLAG-immunoprecipitation followed by Western blotting of the FLAG-immunoprecipitates using the H1.4K85me1 antibody. Results showed a methylation signal in HeLa cells cotransfected with the HA-WHSC1 and FLAG-H1.4-WT vectors, which was abolished in those cotransfected with the HA-Mock and FLAG-H1.4-WT, or those with the HA-WHSC1 and FLAG-H1.4K85A vectors (Fig. 1G).

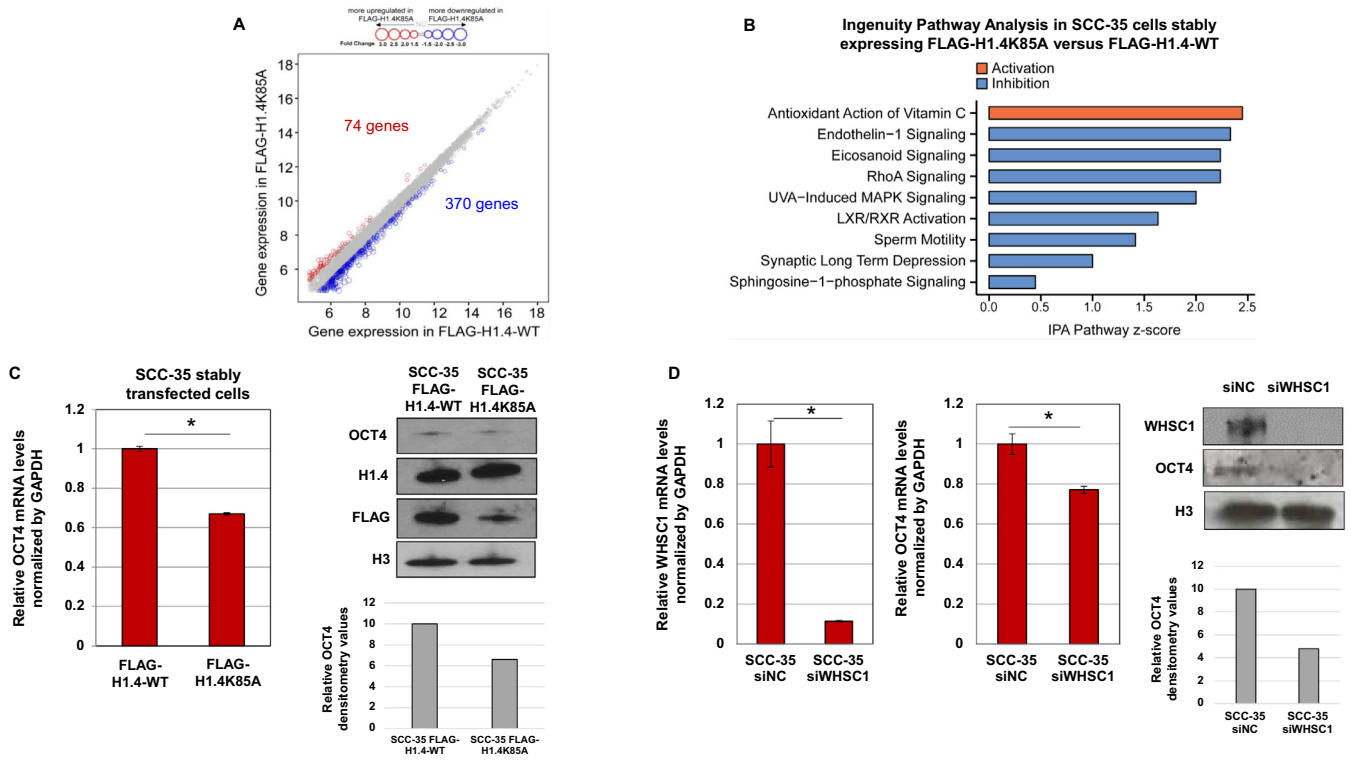

Fig. 2. OCT4 is regulated by H1.4K85 mono-methylation and WHSC1 in SCC-35 cells. A. Differential gene expression analysis in SCC-35 cells stably expressing FLAG-H1.4-WT versus FLAG-H1.4K85A. Y-axis and X-axis represent log2-transformed gene expression levels in FLAG-H1.4K85A and FLAG-H1.4-WT expressing cells respectively. Each circle represents a gene. A total of 11,470 protein-coding genes are shown. Genes that are upregulated ($n = 74$) or downregulated ($n = 370$) by at least 1.5-fold in FLAG-H1.4K85A expressing cells relative to FLAG-H1.4-WT cells are shown in red and blue circles, respectively. The rest of the genes of lesser fold change between the two conditions are shown as grey circles. The size of the circles represents the relative expression fold of change between the two groups. B. Ingenuity canonical pathways enriched in the SCC-35 cells stably transfected with FLAG-H1.4K85A compared to cells transfected with FLAG-H1.4-WT. Data shown for pathways filtered by FDR-corrected $p < 0.20$. C. RT-PCR (left panel) and Western blotting of 8ug of nuclear extract (right panel) for OCT4 in SCC-35 cells stably transfected with FLAG-H1.4-WT versus FLAG-H1.4K85A (*$p < 0.05$, Student t-test, data represented as mean þ SEM of triplicates). Relative densitometry values are also shown. D. RT-PCR for WHSC1 (left panel) and OCT4 (middle panel), and Western blotting (right panel) for WHSC1 (enzymatically active isoform shown, molecular weight 152kD) and OCT4 in 10ug of nuclear extract from parental SCC-35 cells transfected with WHSC1-specific siRNA (RT-PCR in far left panel) *$p < 0.05$, Student t-test, data represented as mean þ SEM of triplicates). Relative densitometry values are also shown. Similar results were obtained in two separate biological replicates.

OCT4 transcription and protein levels are regulated by H1.4K85 mono-methylation and WHSC1 in SCC-35 cells.

To investigate the pathways that are transcriptionally regulated by H1.4K85 mono-methylation in SCCHN cells, we generated SCC-35 cells (with endogenous overexpression of WHSC1) stably expressing FLAG-H1.4-WT or FLAG-H1.4K85A by geneticin (G418) selection. Western blotting of nuclear extracts from the stable cells showed equivalent expression levels of FLAG-H1.4-WT and FLAG-H1.4K85A (Supplementary Fig. S3). Then, we extracted RNA from SCC-35 cells stably expressing either FLAG-H1.4-WT or FLAG-H1.4K85A, and performed RNA-sequencing analysis. From 19,844 protein-coding genes annotated in the GENCODE project [20], we first removed lowly expressed genes (defined as less than 10 reads per condition after normalizing for the library size), leaving 11,470 genes for further analysis. The correlation of gene expression between FLAG-H1.4K85A and FLAG-H1.4-WT was 0.99 (Pearson's correlation, $p < 0.00001$), suggesting that the expression of the great majority of the genes remained unchanged between the two groups (Fig. 2A, grey circles). Next, we focused on genes affected to a larger extent (defined as a fold change of ≥ 1.5 or ≤ -1.5 between the two groups), and 444 genes passed such criteria (Fig. 2A, blue and red circles), hereafter called differentially expressed genes (DEGs). More specifically, results showed that 370 genes were significantly downregulated and 74 genes were upregulated (Supplementary Data, DEGs and pathways) in SCC-35 cells stably expressing FLAG-H1.4K85A compared to FLAG-H1.4-WT, indicating that mono-methylation of H1.4K85 may be predominantly an activating mark. Ingenuity Pathway Analysis (IPA) suggested that pathways related to proliferation, cell death and survival were among the top five IPA diseases and functions affected (Supplementary Table S1). Ingenuity canonical pathways related to cell proliferation were significantly inhibited in SCC-35 cells stably expressing FLAG-H1.4K85A, implying that H1.4K85 mono-methylation may promote the proliferation of head and neck cancer cells (Fig. 2B). Interestingly, using the Ingenuity upstream regulator analysis [20], *OCT4* was one of the top regulators (overlap p-value = 0.04) and was predicted to be inhibited based on the expression changes of 10 downstream target genes regulated by H1.4K85 mono-methylation (Supplementary Fig. S4). Indeed, OCT4 mRNA was downregulated by more than 1.5-fold in SCC-35 cells stably expressing FLAG-H1.4K85A compared to FLAG-H1.4-WT cells, supporting that H1.4K85 mono-methylation may induce transcriptional upregulation of *OCT4* (Supplementary Data, DEGs and pathways). Other

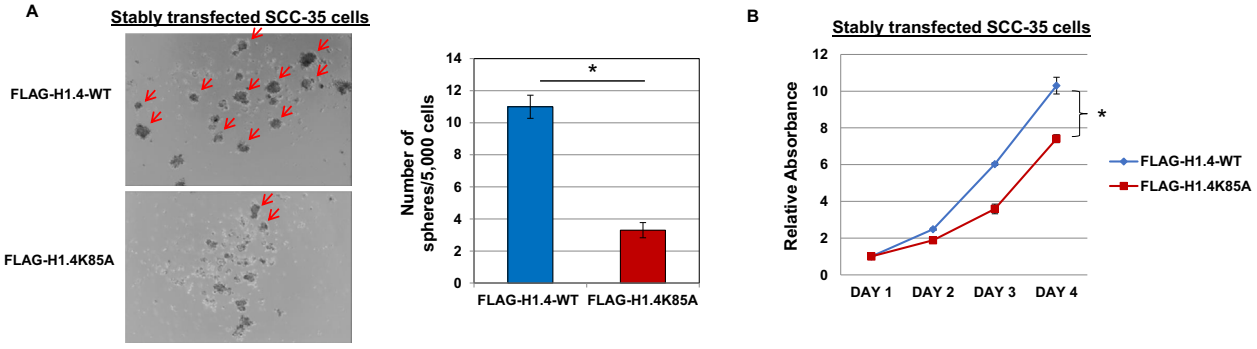

Fig. 3. H1.4K85 mono-methylation increases sphere formation and enhances cell proliferation of SCCHN cells. A. Sphere formation assay of stably transfected SCC-35 SCCHN cells expressing FLAG-H1.4-WT versus FLAG-H1.4K85A constructs. 5000 cells were seeded in 24-well low-attachment plates in serum-free medium supplemented by epidermal growth factor (20 ng/ml). Cells were followed for 7 days and number of spheres was counted in 3 separate wells per condition under the microscope and the mean number of spheres was calculated. Left panel: representative images from one well in each condition. Right panel: histogram of the mean number of spheres from 3 individuals wells in each condition $^*p = 0.001$, Student *t*-test, data represented as mean þ SEM). Similar results were obtained in two different experiments. B. MTT proliferation assays in SCC-35 cells stably expressing FLAG-H1.4-WT versus FLAG-H1.4K85A constructs. 2,000 cells were seeded in 24-well plates in quadruples for each condition. CCK-8 assay was performed at each indicated time point. FLAG-H1.4-WT expressing SCC-35 cells show a significantly higher proliferation rate compared to FLAG-H1.4K85A expressing SCC-35 cells $^*p < 0.05$, Student *t*-test, data represented as mean þ SEM of quadruple values for each time point).

stemness related factors, such as NANOG, SOX2, C-MYC, KLF4, CD44, CD133 and ALDH3A1, were not found to be significantly down-regulated in FLAG-H1.4K85A SCC-35 cells at the mRNA level (Supplementary Data, DEGs and pathways).

Based on our previously published data showing that WHSC1 overexpression is associated with poor differentiation in SCCHN (Saloura et al., 2014) and reports supporting that depletion of linker histones or specific modifications are necessary for the pluripotency of embryonic stem cells ([8,9]), we hypothesized that WHSC1-mediated H1.4K85 mono-methylation may maintain cancer stemness features in SCCHN. Given that OCT4 is a well-known stemness factor, we chose to further investigate OCT4 as a potential downstream target regulated by WHSC1-mediated H1.4K85 mono-methylation. To confirm that *OCT4* is transcriptionally regulated by H1.4K85 mono-methylation, we isolated RNA and validated mRNA expression levels of OCT4 in SCC-35 cells stably expressing either FLAG-H1.4-WT or FLAG-H1.4K85A by PCR analysis. Results confirmed an approximately 40% decrease in OCT4 mRNA levels in SCC-35 cells expressing FLAG-H1.4K85A compared to FLAG-H1.4-WT, indicating that mono-methylation of H1.4K85 may upregulate the expression of OCT4 mRNA (Fig. 2C, left panel). Western blotting of nuclear extracts from the two groups of stably expressing cells also showed a decrease in the OCT4 protein levels in SCC-35 cells stably expressing FLAG-H1.4K85A (Fig. 2C, right panel). Interestingly, we also generated another stably transfected cell line using FaDu cells with endogenously very low levels of WHSC1 (Saloura et al., 2014) and observed no decrease in OCT4 protein levels between the two cell lines (Supplementary Fig. S5). Furthermore, we observed a decrease in OCT4 mRNA and protein levels in parental SCC-35 and PA/CE-PJ15 cells after siRNA-mediated knockdown of WHSC1 (Fig. 2D, Supplementary Fig. S6). The above data support that WHSC1 and H1.4K85 mono-methylation induced by WHSC1 may activate the transcription of *OCT4* in SCCHN cells.

WHSC1-mediated H1.4K85 mono-methylation increases sphere formation and enhances proliferation of SCCHN cells.

Given that OCT4 is a critical stemness factor, we hypothesized that H1.4K85 mono-methylation may induce cancer stemness features in SCCHN cells. To investigate this hypothesis, we assessed whether H1.4K85 mono-methylation enhances sphere formation in SCCHN cells. 5000 SCC-35 cells stably expressing either FLAG-H1.4-WT or FLAG-H1.4K85A were seeded in 24-well low-attachment plates in serum-free medium condition supplemented with epidermal growth factor (20 ng/ml). Cells were monitored for 7 days and the number of spheres per well were counted under a microscope for each condition. Results showed a significantly higher number of spheres formed by SCC-35 cells expressing FLAG-H1.4-WT compared to cells expressing FLAG-H1.4K85A (FLAG-H1.4-WT: mean = 11, FLAG-H1.4K85A: mean = 3.3, Student *t*-test, $p = 0.008$) (Fig. 3A).

To evaluate if H1.4K85 mono-methylation promotes cellular proliferation, we seeded 2000 SCC-35 cells/well stably expressing either FLAG-H1.4-WT or FLAG-H1.4K85A in 24-well plates and performed MTT assays on days 1, 2, 3 and 4 post-seeding. SCC-35 cells stably expressing FLAG-H1.4-WT had a significantly higher proliferation rate compared to cells expressing FLAG-H1.4K85A (Student *t*-test, $p < 0.05$, day 4) (Fig. 3B). In contrast, in stably transfected FaDu cells, we observed no differences in the proliferation rate (Supplementary Fig. S5) and sphere formation assays (data not shown) between the two cell lines. These data indicate that H1.4K85 mono-methylation may play a significant role in promoting stemness in WHSC1 expressing SCCHN cells.

SCC-35-H1.4K85R CRISPR cells have significantly decreased sphere formation and proliferation rate, and decreased expression of OCT4 compared to parental SCC-35 cells.

To further examine whether H1.4K85 mono-methylation induces stemness features in SCCHN cells, we used clustered regularly interspaced short palindromic repeats (CRISPR) to genetically modify the *H1.4* gene (*HIST1H1E*) and introduced a point mutation at H1.4K85, which substituted the lysine at the amino acid position 85 to arginine (K85R) in SCC-35 cells. Sanger sequencing of the *H1.4* gene in SCC-35-H1.4K85R cells revealed three different genotypes (Supplementary Fig. S7); of these, two were predicted to introduce premature stop codons (genotypes II and III) and thus silence *H1.4*, while the third genotype was predicted to transcribe the mutant *H1.4 K85R* gene. Given that SCC-35 cells are tetraploid for the *H1.4* gene, we expected that one or two of the alleles should carry the *K85R* mutations, while two or three of the alleles would be silenced.

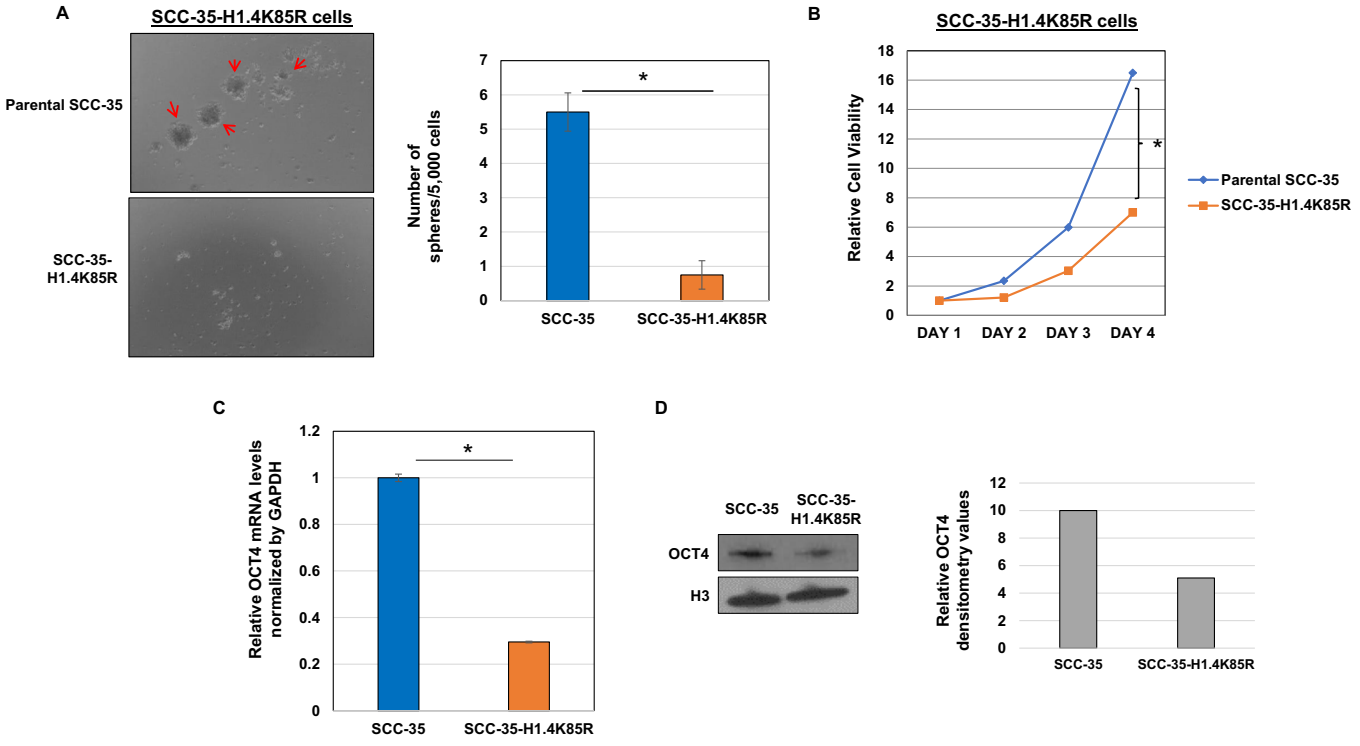

Fig. 4. SCC-35-H1.4K85R CRISPR cells demonstrate decreased sphere formation, proliferation rate, and expression of OCT4 compared to parental SCC-35 cells. A. Sphere formation assay of parental SCC-35 and SCC-35-H1.4K85R cells. 5000 cells were seeded in 24-well low-attachment plates in serum-free medium supplemented by epidermal growth factor (20 ng/ml). Cells were followed for 7 days and number of spheres was counted in 3 separate wells per condition under the microscope and the mean number of spheres was calculated. Left panel: representative images from one well in each condition. Right panel: histogram of the mean number of spheres from 3 individual wells in each condition $^*p = 0.001$, Student *t*-test, data represented as mean þ SEM). Similar results were obtained in two different experiments. B. MTT proliferation assays in parental SCC-35 and SCC-35-H1.4K85R cells. 2,000 cells were seeded in 24-well plates in quadruples for each condition. CCK-8 assay was performed at 2 h at each indicated time point. Parental SCC-35 cells showed a significantly higher proliferation rate compared to SCC-35-H1.4K85R cells $^*p < 0.05$, Student *t*-test, data represented as mean þ SEM of quadruple values for each time point). Similar results were obtained in two different experiments. C. RT-PCR for OCT4 in parental SCC-35 and SCC-35-H1.4K85R cells $^*p < 0.05$, Student *t*-test, data represented as mean þ SEM of triplicate values for each condition). Similar results were obtained in two different experiments. D. Western blotting for OCT4 in parental SCC-35 and SCC-35-H1.4K85R cells. Relative densitometry values are also shown. Similar results were obtained in two different experiments.

RNA-sequencing analysis of the SCC-35-H1.4K85R cells confirmed expression of the H1.4K85R transcript, while the wild-type *H1.4* transcript was not detected. Furthermore, comparison of the total levels of wild-type H1.4 mRNA in the parental SCC-35 cells with those of H1.4K85R mRNA in SCC-35-H1.4K85R cells showed that the latter were approximately 50% of wild-type H1.4 mRNA in parental SCC-35 cells (Supplementary Fig. S8). Other histone H1 variant transcripts, such as H1.2, H1.3 and H1.5, did not incur the K85R point mutation and were detected as wild type (data not shown).

RNA-sequencing showed that SCC-35-H1.4K85R cells had 108 genes downregulated and 66 genes upregulated, implying that H1.4K85 mono-methylation may directly or indirectly regulate the transcription of these genes. Gene set enrichment analysis revealed that the G2M checkpoint and mitotic spindle pathways were predicted to be inhibited in SCC-35-H1.4K85R cells (Supplementary Fig. S9).

We then evaluated the sphere formation capacity and the proliferation rate of SCC-35-H1.4K85R cells compared to parental SCC-35 cells. As expected, SCC-35-H1.4K85R cells formed significantly fewer spheres compared to parental SCC-35 cells (Fig. 4A), similar to the SCC-35 cells stably expressing FLAG-H1.4K85A (Fig. 3A), suggesting that H1.4K85 mono-methylation enables stemness-like characteristics. Accordingly, the proliferation rate of SCC-35-H1.4K85R cells was significantly lower compared to parental cells (Fig. 4B). We then compared the expression levels of OCT4 mRNA in parental SCC-35 and SCC-35-H1.4K85R cells, and found significantly decreased OCT4 mRNA levels in SCC-35-H1.4K85R cells (Fig. 4C). OCT4 protein levels were accordingly decreased in SCC-35-H1.4K85R cells compared to parental SCC-35 cells (Fig. 4D). Interestingly, the total H1.4 protein levels in SCC-35-H1.4K85R cells were decreased compared to the parental SCC-35 cells, consistently with the decrease in the total H1.4 mRNA levels in these cells (Supplementary Fig. S8). H1.5 levels were also decreased. Total H1.2 were stable, while H1.3 levels were increased in SCC-35-H1.4K85R cells, suggesting possible dosage compensation for the decreased H1.4 protein levels in these cells.

Mono-methylated H1.4K85 is enriched and is associated with increased binding of WHSC1 to the OCT4 gene body region in SCC-35 cells.

To investigate the mechanism through which H1.4K85 mono-methylation induces transcriptional upregulation of *OCT4*, we conducted chromatin immunoprecipitation using a FLAG antibody in SCC-35 cells 48 h after transient transfection with either FLAG-H1.4-WT or

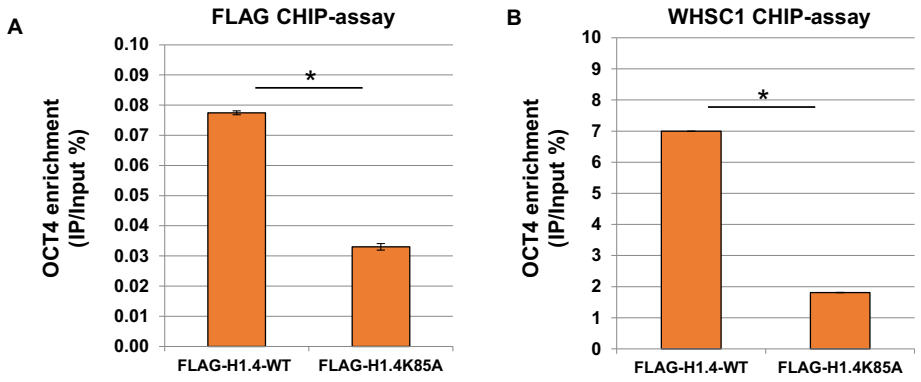

Fig. 5. Mono-methylated H1.4K85 is enriched and is associated with increased binding of WHSC1 to the *OCT4* gene body region in SCC-35 cells. A. CHIP-assay for FLAG-H1.4-WT versus FLAG-H1.4K85A using an anti-FLAG antibody (F3165) followed by RT-PCR for OCT4. SCC-35 cells were transiently transfected with FLAG-H1.4-WT versus FLAG-H1.4K85A vectors. Nuclear extraction was conducted and chromatin immunoprecipitation followed by RT-PCR for OCT4 was performed *p-value <0.05, Student t-test, data represented as mean þ SEM of triplicates). B. CHIP-assay for WHSC1 in SCC-35 cells stably transfected to express FLAG-H1.4-WT versus FLAG-H1.4K85A using a WHSC1 antibody (Abcam 75359) in nuclear extracts, followed by RT-PCR for OCT4 *p-value <0.05, Student t-test, data represented as mean þ SEM of triplicates).

FLAG-H1.4K85A (Supplementary Fig. S10). We found enrichment of FLAG-H1.4-WT in the *OCT4* gene body region compared to FLAG-H1.4K85A, indicating that the absence of H1.4K85 mono-methylation may be associated with decreased transcription of the *OCT4* gene (Fig. 5A). To assess whether the binding of WHSC1 is also enabled by higher levels of H1.4K85 mono-methylation in the *OCT4* gene body region, we conducted chromatin immunoprecipitation in the stably transfected cells using a WHSC1 antibody and found significant enrichment of WHSC1 in the *OCT4* gene body region in SCC-35 cells stably expressing FLAG-H1.4-WT compared to those with FLAG-H1.4K85A (Fig. 5B).

Discussion

Linker histones are evolutionarily conserved proteins that are essential for the organization, higher order structure, spatial arrangement and stability of chromatin within the nucleus of all eukaryotic cells. They are mostly known to impact the architectural organization of chromatin, but their roles in epigenetic regulation are not well clarified. While linker histones are subject to various post-translational modifications, the enzymes that impart these modifications as well as the functions of these modifications are not well described [21].

In this study, we show that WHSC1 interacts with linker histone H1 in SCCHN cells and that it directly mono-methylates it at lysine 85 (H1K85) in its globular domain, providing the first evidence of a non-H3K36 substrate of WHSC1. Our mass spectrometry analysis showed that WHSC1 could interact with all linker histone variants (H1.1, H1.2, H1.3, H1.4 and H1.5) with coverage rates ranging from 30-40%. We decided to focus on variant H1.4 because it is the most highly expressed linker histone variant in somatic cells, and together with H1.2, it showed higher expression levels in SCCHN cells compared to other H1 variants. To investigate the biological role of H1K85 mono-methylation, we generated SCC-35 cells (with endogenous overexpression of WHSC1) stably expressing either FLAG-H1.4-WT or FLAG-H1.4K85A constructs. RNA-sequencing of these cell lines showed that 370 genes were downregulated and 75 genes were upregulated in the FLAG-H1.4K85A cells, signifying that H1.4K85 mono-methylation may function predominantly as an activating mark. Ingenuity Pathway analysis revealed that pathways related to cell proliferation and survival are inhibited and OCT4 was significantly downregulated in FLAG-H1.4K85A cells. Consistent with the prominent role of OCT4 as a stemness factor, FLAG-H1.4K85A cells formed significantly fewer spheres and had a lower proliferation rate compared to their wild-type counterparts.

We then used a second cell line model of SCC-35 cells that were genetically modified using CRISPR to express H1.4K85R, which cannot get methylated at H1.4K85. RNA-sequencing followed by gene set enrichment analysis revealed that the G2M checkpoint and mitotic spindle pathways had significantly negative enrichment scores in SCC-35-H1.4K85R cells, consistent with the decreased proliferation rate of these cells. Consistently with the stably transfected cells, OCT4 mRNA and protein levels were decreased in SCC-35-H1.4K85R cells which also showed significantly impaired ability to form spheres compared to parental SCC-35 cells. Finally, our CHIP assays showed that both WHSC1 and FLAG-H1.4-WT, which can get methylated at K85, were enriched in the *OCT4* gene body region, while knockdown of WHSC1 in SCC-35 cells was associated with decreased OCT4 mRNA and protein levels, supporting the importance of WHSC1 and H1.4K85 mono-methylation in the transcriptional regulation of this gene.

Given the prominent role of linker histones in chromatin organization and transcriptional accessibility, we assessed whether H1.4K85 mono-methylation has an effect on the degree of chromatin compaction using a micrococcal nuclease assay in parental SCC-35 compared to SCC-35-H1.4K85R cells. We chose these cell lines to assess whether mono-methylation of H1.4K85 affects chromatin condensation because the levels of expression of H1 were more physiological compared to the stably transfected SCC-35 cells. Interestingly, we did not observe any differences in chromatin digestion between parental SCC-35 cells and SCC-35-H1.4K85R cells (Supplementary Fig. S11). This finding is not completely unexpected, given that methylation of lysine residues is not known to affect the electrostatic charge of lysines and thus their binding to DNA. Another possible reason for our finding may be the observed dosage compensation through H1.3 in the SCC-35-H1.4K85R cells (Fig. 4D). More specifically, while all H1.4 transcripts were mutant H1.4K85R, the total H1.4 protein levels in SCC-35-H1.4K85R cells were decreased (due to silencing of some of the *H1.4* alleles), and thus dosage compensation through wild-type H1.3 may have ensued. As we cannot exclude that WHSC1 may mono-methylate all H1 variants at K85, the overexpressed H1.3 may be mono-methylated at K85, which would compensate for the decreased H1.4K85 mono-methylation levels in SCC-35-H1.4K85R cells. If that is the case, it may be precarious to draw any conclusions on the effect of methylation of H1.4K85 on chromatin accessibility using this cell line.

The importance of H1K85 for the interaction of H1 with the DNA to facilitate chromatin condensation has already been reported. More specifically, a previous study showed that substitution of K85 of $H1^0$ with alanine, a hydrophobic residue, in murine cells decreased the binding affinity of $H1^0$ to nucleosomes *in vivo*, underlining the importance of H1K85 in stabilizing the nucleosome [22]. In another study, H1K85 acetylation by the acetyltransferase P300/CBP-associated factor (PCAF) induced chromatin condensation in HeLa cells by promoting the interaction of linker histone H1 with core histones and the heterochromatin protein 1 [23]. In the same study, authors showed that H1.4 knockout HeLa cells stably transfected to express FLAG-H1.4 K85R had greater degree of chromatin digestion compared to H1.4 knockout HeLa cells stably transfected with FLAG-H1.4 WT in a micrococcal nuclease assay, however, this difference was attributed to acetylation of H1.4K85 by PCAF, which induced chromatin condensation. While we did not find any differences in the chromatin condensation between parental SCC-35 and SCC-35-H1.4K85R cells, it is possible that some modifications on the same residues of linker histones may stabilize chromatin, while others may regulate gene expression. Furthermore, a specific residue may be amenable to different modifications in different cell types.

A recent study [26] showed that a subset of HPV-negative head and neck cancer patients that carry H3K36M mutations (lysine 36 of histone H3 substituted to methionine that cannot get methylated) have significantly decreased to absent H3K36me2 levels and tend to suppress the expression of genes involved in epidermal differentiation and keratinization processes. This finding contradicted our previously published results (Saloura et al., 2014) showing that higher H3K36me2 protein levels in head and neck cancer tumor samples were associated with poor differentiation. Our findings of the presented work suggest that WHSC1 may promote stemness-like features through a different pathway, that is H1.4K85 methylation, however, the question of whether WHSC1-mediated H3K36me2 may also promote stemness in head and neck cancer merits further investigation.

A significant shortcoming of this study is that we could not detect endogenous levels of H1.4K85 mono-methylation in our two cell line models using the H1.4K85 mono-methylation custom-made antibody (ST0812). Furthermore, we could not immunoprecipitate endogenous H1.4 protein to assess endogenous H1.4K85 mono-methylation levels despite multiple attempts with four commercially available antibodies. Additionally, we could not evaluate the presence of H1.4K85 mono-methylation in patient samples given that our custom-made antibody recognized multiple bands in cellular protein extracts.

In conclusion, this is the first report describing the mono-methylation of linker histone at K85 and its function in SCCHN cells. We also show that this methylation is mediated by the protein methyltransferase WHSC1 which is known to di-methylate lysine 36 of histone H3, making this the first report of a novel substrate for WHSC1. WHSC1 has been shown to be significantly overexpressed in squamous cell carcinomas of the head and neck (Saloura et al., 2014). Our study supports that WHSC1 mono-methylates H1K85 and this methylation enables stemness features in SCCHN cells, providing biological rationale to target WHSC1 in squamous cell carcinoma of the head and neck.

Acknowledgements

This project was supported by an Institutional Research Grant (#IRG-58-004-53-IRG) from the American Cancer Society and the Cancer Center Support Grant (#P30 CA14599) of the University of Chicago Medicine Comprehensive Cancer Center. We would also like to acknowledge Thomas A. Johnson (Laboratory of Receptor Biology and Gene Expression, National Cancer Institute) for his critical input on this work.

Appendix A. Supplementary data

Supplementary data to this article can be found online at https://doi.org/10.1016/j.neo.2020.05.002.

References

1. Hendzel MJ, Lever MA, Crawford E, Th'ng JP. The C-terminal domain is the primary determinant of histone H1 binding to chromatin in vivo. *J Biol Chem.* 2004;**279**(19):20028–34, PMID: 14985337.
2. Sancho M, Diani E, Beato M, Jordan A. Depletion of human histone H1 variants uncovers specific Roles in gene expression and cell growth. PLoS Genet 2008;4(10):e1000227. PMCID: PMC2563032.
3. Allan J, Cowling GJ, Harborne N, Cattini P, Craigie R, Gould H. Regulation of the higher-order structure of chromatin by histones H1 and H5. J Cell Biol. 1981;90(2):279-88. PMCID: PMC2111872.
4. Happel N, Doenecke D. Histone H1 and its isoforms: contribution to chromatin structure and function. *Gene* 2009;**431**(1–2):1–12, PMID: 19059319.
5. Robinson PJ, Rhodes D. Structure of the `30 nm' chromatin fibre: a key role for the linker histone. *Curr Opin Struct Biol* 2006;**16**(3):336–43, PMID: 16714106.
6. Herrera RE, Chen F, Weinberg RA. Increased histone H1 phosphorylation and relaxed chromatin structure in Rb-deficient fibroblasts. *Proc. Natl. Acad. Sci.* 1996;**93**(21):11510–5, PMCID: PMC38088.
7. Zlatanova J, Doenecke D. Histone H1 zero: a major player in cell differentiation?. *FASEB J* 1994;**8**(15):1260–8, PMID: 8001738.
8. Zhang Y et al. Histone H1 depletion impairs embryonic stem cell differentiation. PLoS Genet 2012;8:e1002691. PMCID: PMC3349736.
9. Christophorou MA, Castelo-Branco G, Halley-Stott RP, Oliveira CS4, Loos R, Radzisheuskaya A, Mowen KA7, Bertone P, Silva JC, Zernicka-Goetz M9, Nielsen ML, Gurdon JB, Kouzarides T. Citrullination regulates pluripotency and histone H1 binding to chromatin. Nature 2014;507(7490):104–8. PMID: 24463520..
10. Konishi A, Shimizu S, Hirota J, Takao T, Fan Y, Matsuoka Y, Zhang L, Yoneda Y, Fujii Y, Skoultchi AI, Tsujimoto Y. Involvement of histone H1.2 in apoptosis induced by DNA double-strand breaks. Cell 2003;114(6):673–88. PMID: 14505568..
11. Garg M, Ramdas N, Vijayalakshmi M, Shivashankar GV, Sarin A. The C-terminal domain (CTD) in linker histones antagonizes anti-apoptotic proteins to modulate apoptotic outcomes at the mitochondrion. Cell Death Dis 2014;5:e1058. PMCID: PMC3944238..
12. Raghuram N, Carrero G, Th'ng J, Hendzel MJ. Molecular dynamics of histone H1. *Biochem Cell Biol* 2009;**87**(1):189–206, PMID: 19234534.
13. Wood C, Snijders A, Williamson J, Reynolds C, Baldwin J, Dickman M. Post-translational modifications of the linker histone variants and their association with cell mechanisms. *FEBS J* 2009;**276**(14):3685–97, PMID: 19490123.
14. Chadee DN, Peltier CP, Davie JR. Histone H1(S)-3 phosphorylation in Ha-ras oncogene transformed mouse fibroblasts. *Oncogene* 2002;**21**(55):8397–403, PMID: 12466960.
15. Murga M, Jaco I, Fan Y, Soria R, Martinez-Pastor B, Cuadrado M, Yang SM, Blasco MA, Skoultchi AI, Fernandez-Capetillo O. Global chromatin compaction limits the strength of the DNA damage response. J Cell Biol 2007;178(7):1101–8. PMCID: PMC2064646.
16. Cerami E, Gao J, Dogrusoz U, Gross BE, Sumer SO, Aksoy BA, Jacobsen A, Byrne CJ, Heuer ML, Larsson E, Antipin Y, Reva B, Goldberg AP, Sander C, Schultz N. The cBio cancer genomics portal: an open platform for exploring multidimensional cancer genomics data. Cancer Discov 2012;2(5):401–4. PMCID: PMC3956037..
17. Li H, Kaminski MS, Li Y, Yildiz M, Ouillette P, Jones S, Fox H, Jacobi K, Saiya-Cork K, Bixby D, Lebovic D, Roulston D, Shedden K, Sabel M, Marentette L, Cimmino V, Chang AE, Malek SN. Mutations in linker histone genes HIST1H1 B, C, D, and E; OCT2 (POU2F2); IRF8; and ARID1A underlying the pathogenesis of follicular lymphoma. *Blood* 2014;**123**(10):1487–98, PMID: 24435047.
18. Chaturvedi AK, Anderson WF, Lortet-Tieulent J, Curado MP, Ferlay J, Franceschi S, Rosenberg PS, Bray F, Gillison ML. Worldwide trends in incidence rates for oral cavity and oropharyngeal cancers. *J Clin Oncol* 2013;**31**(36):4550–9.

19. Saloura V, Cho HS, Kyiotani K, Alachkar H, Zuo Z, Nakakido M, Tsunoda T, Seiwert T, Lingen M, Licht J, Nakamura Y, Hamamoto R. WHSC1 Promotes Oncogenesis through Regulation of NIMA related-kinase-7 in Squamous Cell Carcinoma of the Head and Neck. Mol Cancer Res 2014. pii: molcanres.0292.2014. PMID: 25280969.
20. Harrow J, Frankish A, Gonzalez JM, Tapanari E, Diekhans M, Kokocinski F, Aken BL, Barrell D, Zadissa A, Searle S, Barnes I, Bignell A, Boychenko V, Hunt T, Kay M, Mukherjee G, Rajan J, Despacio-Reyes G, Saunders G, Steward C, Harte R, Lin M, Howald C, Tanzer A, Derrien T, Chrast J, Walters N, Balasubramanian S, Pei B, Tress M, Rodriguez JM, Ezkurdia I, van Baren J, Brent M, Haussler D, Kellis M, Valencia A, Reymond A, Gerstein M, GuigÆ R, Hubbard TJ. GENCODE: the reference human genome annotation for The ENCODE Project. *Genome Res* 2012;**22**(9):1760–74. https://doi.org/10.1101/gr.135350.111.
21. Fyodorov DV, Zhou BR, Skoultchi AI, Bai Y. Emerging roles of linker histones in regulating chromatin structure and function. *Nat Rev Mol Cell Biol* 2018;**19**(3):192–206. https://doi.org/10.1038/nrm.2017.94, Epub 2017 Oct 11.
22. Brown DT, Izard T, Misteli T. Mapping the interaction surface of linker histone H1(0) with the nucleosome of native chromatinin vivo. *Nat Struct Mol Biol* 2006;**13**(3):250–5, Epub 2006 Feb 5.
23. Li Y, Li Z, Dong L, Tang M, Zhang P, Zhang C, Cao Z, Zhu Q, Chen Y, Wang H, Wang T, Lv D, Wang L, Zhao Y, Yang Y, Wang H, Zhang H, Roeder RG, Zhu WG. Histone H1 acetylation at lysine 85 regulates chromatin condensation and genome stability upon DNA damage. *Nucleic Acids Res* 2018;**46**(15):7716–30. https://doi.org/10.1093/nar/gky568.
24. Matson V, Fessler J, Bao R, Chongsuwat T, Zha Y, Alegre ML, Luke JJ, Gajewski TF. The commensal microbiome is associated with anti-PD1 efficacy in metastatic melanomapatients. *Science* 2018;**359**(6371):104–8. https://doi.org/10.1126/science.aao3290.
25. Frankish A, Diekhans M, Ferreira AM, Johnson R, Jungreis I, Loveland J, et al. GENCODE reference annotation for the human and mouse genomes. *Nucleic Acids Res* 2019;**47**(D1):D766–73. https://doi.org/10.1093/nar/gky955.
26. Papillon-Cavanagh S, Lu C, Gayden T, Mikael LG, Bechet D, Karamboulas C, Ailles L, Karamchandani J, Marchione DM, Garcia BA, Weinreb I, Goldstein D, Lewis PW, Dancu OM, Dhaliwal S, Stecho W, Howlett CJ, Mymryk JS, Barrett JW, Nichols AC, Allis CD, Majewski J, Jabado N. Impaired H3K36 methylation defines a subset of head and neck squamous cell carcinomas. Nat Genet 2017;49(2):180–185. doi: 10.1038/ng.3757..